Acta Mech 226, 1267–1281 (2015)
DOI 10.1007/s00707-014-1249-3

George C. Tsiatas · Aristophanes J. Yiotis

Size effect on the static, dynamic and buckling analysis of orthotropic Kirchhoff-type skew micro-plates based on a modified couple stress theory: comparison with the nonlocal elasticity theory

Received: 21 March 2014 / Revised: 19 September 2014 / Published online: 14 October 2014

Abstract The size effect on orthotropic Kirchhoff-type skew micro-plates is investigated based on a modified couple stress theory. For a three-dimensional orthotropic body, three additional material length scale parameters should be involved in the modified couple stress theory (with respect to the three shear moduli). However, in this study and without restricting the generality, we assume that the 2D couple stress state of the orthotropic micro-plate is described solely by only one material length scale parameter in accordance with the in-plane shear modulus. Furthermore, this reasonable assumption allows us to compare qualitatively the results with those obtained by the nonlocal elasticity theory, which also uses only one material length scale parameter to capture the size effect. Using Hamilton's principle, the governing equilibrium equation of the micro-plate and the associated general boundary conditions are derived in terms of the deflection. The resulting initial boundary value problem is of fourth order, and it is solved employing the analog equation method. Example problems are presented for orthotropic skew micro-plates, and useful conclusions are drawn from the investigation of their micron-scale response. Some of the findings detected in studying the microstructure vibratory response of orthotropic skew micro-plates, based on the modified couple stress theory, are also verified by those obtained by the nonlocal elasticity theory. Nevertheless, a new important finding is that both the frequency and critical load parameters increase by increasing the material length scale parameter of the modified couple stress theory, which is in direct contradiction to that of the nonlocal elasticity theory where these parameters decrease by increasing the nonlocal parameter.

1 Introduction

Thin plates are structural components, which have been widely used in micro and nanotechnology. The behavior of such structures has been proven experimentally to be size dependent (e.g., see [1]) leading to the insufficiency of the classical theories. Thus, the recourse to higher-order theories containing internal material length scale parameters is inevitable. In the present study, we focus on materials which exhibit orthotropy (e.g., silicon, graphene sheets, honeycomb), a case that is frequently encountered in the analysis of nanoplates [2].

Although many scholars have studied the micron-response of thin isotropic micro-plates, employing various higher-order elasticity theories [3–9], the work that has been reported on the subject of orthotropic micro-plates is limited only to analytical approaches for free vibration and buckling analysis of nanoplates of graphene sheet, employing the nonlocal elasticity theory of Eringen [10]. More specifically, Sakhaee-Pour [11] studied the

G. C. Tsiatas (✉) · A. J. Yiotis
Institute of Structural Analysis and Seismic Research, School of Civil Engineering,
National Technical University of Athens, 15773 Athens, Greece
E-mail: gtsiatas@gmail.com
URL:http://users.ntua.gr/gtsiatas

A. J. Yiotis
E-mail: fgiotis@otenet.gr

elastic buckling problem of a single-layered graphene sheet, while Pradhan and Phadikar [12] carried out the vibration analysis of embedded multilayered graphene sheets and Murmu and Pradhan [13] solved the buckling problem of a single-layered graphene sheet. Furthermore, Pouresmaeeli et al. [14] presented an analytical approach for free vibration of all edges simply supported double-orthotropic nanoplates, Satish et al. [15] investigated the free vibrations of orthotropic nanoplates using the two variable refined plate theory and nonlocal continuum mechanics for small-scale effects and Pouresmaeeli et al. [16] studied the vibration characteristics of a simply supported viscoelastic nanoplate by including the effect of a viscoelastic foundation. The only numerical methods that have been employed so far are the differential quadrature method (DQM) [17–19] for the investigation of the vibration and buckling response of orthotropic single-layered graphene sheet using the nonlocal elasticity theory, the finite element method (FEM) by Shahidi et al. [20] for the vibration analysis of orthotropic nanoplates with arbitrary variation in thickness based also on the nonlocal continuum theory, the finite strip method by Analooei et al. [21] for the buckling and vibration analyses of orthotropic nanoplates using nonlocal continuum mechanics and the boundary element method (BEM) by Tsiatas and Yiotis [22] for the static analysis of microstructure-dependent rectangular and elliptical orthotropic plates based on the modified couple stress theory of Yang et al. [23,24].

To the best of the authors' knowledge, the investigation of the microstructure response of orthotropic skew plates is restricted only to the works of Malekzadeh et al. [25] and Alibeygi Beni and Malekzadeh [26] who studied the nonlocal free vibrations of orthotropic arbitrary straight-sided quadrilateral and skew nanoplates based on the first-order shear deformation theory (FSDT) in conjunction with DQM.

In this work, the size effect on orthotropic Kirchhoff-type skew micro-plates is studied based on the modified couple stress theory developed by Yang et al. [23]. In this modified, couple stress theory, an additional equilibrium relation (moments of couples) forces the couple stress tensor to be symmetric. Therefore, the strain energy comprises the symmetric stress tensor (conjugate to strain tensor) and the deviatoric part of the couple stress tensor (conjugate to curvature tensor) as it was already mentioned by Antoine [27]. Although, for a three-dimensional (3D) orthotropic body, three additional length scale parameters should be involved in the couple stress theory (with respect to the three shear moduli), in this study and without restricting the generality, we assume that the 2D couple stress state of the orthotropic micro-plate is described solely by only one material length scale parameter in accordance with the in-plane shear modulus [22]. Furthermore, this reasonable assumption allows us to compare qualitatively the results with those obtained by the nonlocal elasticity theory, which also uses only one material length scale parameter to capture the size effect [25,26]. However, in the newly published article by Chen and Li [28], an anisotropic laminated Kirchhoff plate model with two material length scale parameters is proposed—based on the modified couple stress theory of Yang et al. [23]—which relates implausibly the symmetric couple stress moment tensor to the asymmetric curvature tensor. In their work, Chen and Li [28] present constitutive relations for anisotropic elasticity, which are mistakenly presumed to be published by Koiter [29].

In this paper, the governing equilibrium equation of an orthotropic skew micro-plate and the associated general boundary conditions in terms of the deflection are derived using Hamilton's principle. The resulting initial boundary value problem of the micro-plate is of fourth order, and it is solved using the analog equation method (AEM). Numerical results for orthotropic skew and rectangular plates of various aspect ratios subjected to vibratory or compressive in-plane forces are presented, and useful conclusions are drawn from the investigation of their micron-scale response. Some of the findings detected in studying the microstructure vibratory response of orthotropic skew micro-plates, based on the modified couple stress theory, are also verified by those obtained by the nonlocal elasticity theory. Nevertheless, a new important finding is that both the frequency and critical load parameters increase with increasing the material length scale parameter of the modified couple stress theory, which is in direct contradiction to that of the nonlocal elasticity theory where these parameters decrease with increasing the nonlocal parameter [21,25,26]. As far as it concerns the vibration case, Santos and Reddy [30] came to the same conclusion studying the vibration of Timoshenko beams using nonclassical elasticity theories. They reported that the nonlocal natural frequencies are found to be lower than the classical ones, while the natural frequencies estimated by the modified couple stress theory are higher.

2 Problem formulation

Without restricting the generality, we consider a thin elastic skew plate occupying the two-dimensional domain Ω in the x, y plane bounded by the boundary Γ (see Fig. 1a) consisting of homogeneous orthotropic linearly elastic material, having thickness h and surface mass density $\rho(\mathbf{x})$ with $\mathbf{x} : (x, y) \in \Omega$. The plate is deflected

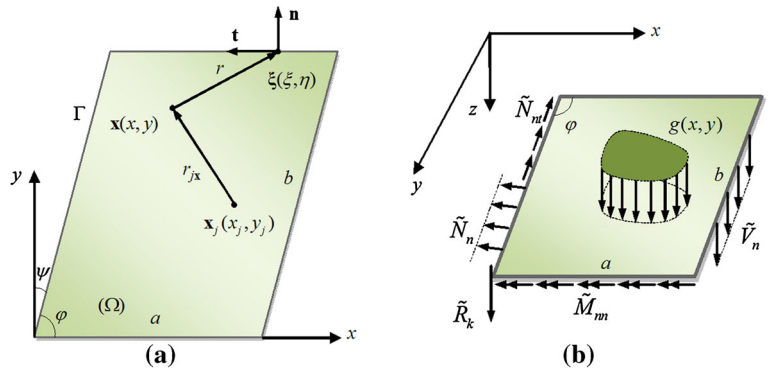

Fig. 1 **a** Plate geometry and notation, **b** loads acting on the plate

under the combined action of the distributed transverse loading $g(\mathbf{x})$ with $\mathbf{x} : (x, y) \in \Omega$ and the edge loads $\tilde{N}_n(\mathbf{x})$, $\tilde{N}_{nt}(\mathbf{x})$, $\tilde{M}_{nn}(\mathbf{x})$ and $\tilde{V}_n(\mathbf{x})$ with $\mathbf{x} : (x, y) \in \Gamma$ (see Fig. 1b). The deformation state at any point through the plate thickness is described by [31]

$$\bar{u}(x, y, z) = u(x, y) - zw_{,x}, \tag{1}$$
$$\bar{v}(x, y, z) = v(x, y) - zw_{,y}, \tag{2}$$
$$\bar{w}(x, y, z, t) = w(x, y, t) \tag{3}$$

where u and v are the in-plane displacements, and w is the transverse deflection of the middle surface. Taking into account the aforementioned displacement field and following Tsiatas [5], the displacement and rotation vectors of the micro-plate become

$$\mathbf{u} = (u - zw_{,x})\,\mathbf{e}_1 + \left(v - zw_{,y}\right)\mathbf{e}_2 + w\mathbf{e}_3, \tag{4}$$
$$\boldsymbol{\theta} = w_{,y}\,\mathbf{e}_1 - w_{,x}\,\mathbf{e}_2 + \tfrac{1}{2}\left(v_{,x} - u_{,y}\right)\mathbf{e}_3, \tag{5}$$

respectively, while the nonzero components of the strain and curvature tensor take the following form:

$$\varepsilon_x = u_{,x} - zw_{,xx}, \quad \varepsilon_y = v_{,y} - zw_{,yy}, \quad \gamma_{xy} = u_{,y} + v_{,x} - 2zw_{,xy}, \tag{6.1–3}$$

$$\chi_x = w_{,xy}, \quad \chi_y = -w_{,xy}, \quad \chi_{xy} = \frac{1}{2}\left(w_{,yy} - w_{,xx}\right), \tag{7.1–3}$$

$$\chi_{xz} = \frac{1}{4}\left(v_{,xx} - u_{,xy}\right), \quad \chi_{yz} = \frac{1}{4}\left(v_{,xy} - u_{,yy}\right). \tag{7.4,5}$$

In the general case of a three-dimensional (3D) orthotropic body, the constitutive relations contain nine independent moduli. These materials have three orthogonal planes of elastic symmetry and are usually defined by the constants: E_1, E_2, E_3 (Young's moduli), $\nu_{12}, \nu_{13}, \nu_{23}$ (Poisson's ratios) and G_{12}, G_{13}, G_{23} (Shear moduli) [32]. Nevertheless, many scholars (e.g., Kirchhoff, Mindlin, Reddy) have developed two-dimensional (2D) theories for plate structures based on kinematic assumptions which take into consideration that the plate thickness is very small compared to the other two dimensions.

In the orthotropic Kirchhoff-type plate theory, the linear constitutive equations for a 2D state of plane stress have the following form [33]:

$$\sigma_x = C_{11}\varepsilon_x + C_{12}\varepsilon_y = \frac{E_1}{1 - \nu_{12}\nu_{21}}\varepsilon_x + \frac{\nu_{12}E_2}{1 - \nu_{12}\nu_{21}}\varepsilon_y, \tag{8.1}$$
$$\sigma_y = C_{12}\varepsilon_x + C_{22}\varepsilon_y = \frac{\nu_{12}E_2}{1 - \nu_{12}\nu_{21}}\varepsilon_x + \frac{E_2}{1 - \nu_{12}\nu_{21}}\varepsilon_y, \tag{8.2}$$
$$\sigma_{xy} = C_{66}\gamma_{xy} = G_{12}\gamma_{xy} \tag{8.3}$$

with $\nu_{12}E_2 = \nu_{21}E_1$. Furthermore, in the modified couple stress theory, proposed by Yang et al. [23], the constitutive equations are relations between the deviatoric part of the couple stress tensor and the curvature tensor. In this study, without restricting the generality, we assume that the aforementioned relations have the following form [22]:

$$m_x = 2G_{12}l^2\chi_x, \quad m_y = 2G_{12}l^2\chi_y, \quad m_{xy} = 2G_{12}l^2\chi_{xy}, \tag{9.1–3}$$

$$m_{xz} = 2G_{12}l^2\chi_{xz}, \quad m_{yz} = 2G_{12}l^2\chi_{yz} \tag{9.4,5}$$

with l being the material length scale parameter. That is, the 2D couple stress state of the orthotropic micro-plate is described solely by only one material length scale parameter in accordance with the in-plane shear modulus G_{12} [22]. Furthermore, this reasonable assumption allows us to compare qualitatively the results with those obtained by the nonlocal elasticity theory, which also uses only one material length scale parameter to capture the size effect [25,26].

The strain energy of the orthotropic Kirchhoff-type micro-plate is written as

$$\begin{aligned} U &= \frac{1}{2}\int_{\Omega}\int_{-h/2}^{h/2}\left(\sigma_x\varepsilon_x + \sigma_y\varepsilon_y + \sigma_{xy}\gamma_{xy} + m_x\chi_x + m_y\chi_y + 2m_{xy}\chi_{xy} + 2m_{xz}\chi_{xz} + 2m_{yz}\chi_{yz}\right)\mathrm{d}z\mathrm{d}\Omega \\ &= \frac{1}{2}\int_{\Omega}\Big[N_x u_{,x} + N_y v_{,y} + N_{xy}\left(u_{,y} + v_{,x}\right) + N_x\left(w_{,x}\right)^2 + 2N_{xy}w_{,x}\,w_{,y} + N_y\left(w_{,y}\right)^2 - M_x w_{,xx} \\ &\quad - M_y w_{,yy} + 2M_{xy}w_{,xy} + Y_x w_{,xy} - Y_y w_{,xy} + Y_{xy}\left(w_{,yy} - w_{,xx}\right) + Y_{xz}\frac{1}{2}\left(v_{,xx} - u_{,xy}\right) \\ &\quad + Y_{yz}\frac{1}{2}\left(v_{,xy} - u_{,yy}\right)\Big]\mathrm{d}\Omega \end{aligned} \tag{10}$$

where N_x, N_y, N_{xy} are the membrane forces, M_x, M_y, M_{xy} are the bending moments, and Y_x, Y_y, Y_{xy}, Y_{xz}, Y_{yz} are the couple moments defined as

$$\begin{Bmatrix} N_x \\ N_y \\ N_{xy} \end{Bmatrix} = \int_{-h/2}^{h/2}\begin{Bmatrix} \sigma_x \\ \sigma_y \\ \sigma_{xy} \end{Bmatrix}\mathrm{d}z, \quad \begin{Bmatrix} M_x \\ M_y \\ M_{xy} \end{Bmatrix} = \int_{-h/2}^{h/2}\begin{Bmatrix} \sigma_x \\ \sigma_y \\ -\sigma_{xy} \end{Bmatrix} z\mathrm{d}z,$$
$$\begin{Bmatrix} Y_x \\ Y_y \\ Y_{xy}, Y_{xz}, Y_{yz} \end{Bmatrix} = \int_{-h/2}^{h/2}\begin{Bmatrix} m_x \\ m_y \\ m_{xy}, m_{xz}, m_{yz} \end{Bmatrix}\mathrm{d}z. \tag{11.1–3}$$

Substituting Eqs. (8) and (9) into Eqs. (11) the latter become

$$N_x = C_{11}u_{,x} + C_{12}u_{,y}, \quad N_y = C_{12}u_{,x} + C_{22}u_{,y}, \quad N_{xy} = C_{66}\left(u_{,y} + v_{,x}\right), \tag{12.1–3}$$

$$M_x = -D_{11}w_{,xx} - D_{12}w_{,yy}, \quad M_y = -D_{22}w_{,yy} - D_{12}w_{,xx}, \quad M_{xy} = 2D_{66}w_{,xy}, \tag{13.1–3}$$

$$Y_x = 2D^l w_{,xy}, \quad Y_y = -2D^l w_{,xy}, \quad Y_{xy} = D^l\left(w_{,yy} - w_{,xx}\right), \tag{13.4–6}$$

$$Y_{xz} = \frac{1}{2}D^l\left(v_{,xx} - u_{,xy}\right), \quad Y_{yz} = \frac{1}{2}D^l\left(v_{,xy} - u_{,yy}\right) \tag{13.7,8}$$

where $D_{ij} = C_{ij}h^3/12$ are the orthotropic plate rigidities and $D^l = l^2G_{12}h$ is the contribution of rotation gradients to the bending rigidity [5].

The kinetic energy, neglecting the in-plane inertia forces, is given by

$$K = \frac{1}{2}\int_{\Omega} \rho\left(\mathbf{x}\right)\dot{w}^2 \mathrm{d}\Omega. \tag{14}$$

Here, the dot designates differentiation with respect to time. The potential energy due to applied loads is

$$W = -\int_{\Omega} g\left(\mathbf{x},t\right) w \mathrm{d}\Omega - \int_{\Gamma}\left(\tilde{N}_n u_n + \tilde{N}_{nt} u_t\right)\mathrm{d}s + \int_{\Omega}\tilde{M}_{nn} w_{,n}\,\mathrm{d}s - \int_{\Omega}\tilde{V}_n w \mathrm{d}s \tag{15}$$

where u_n and u_t are the normal and tangential displacements at the boundary Γ.

The Hamilton's principle, which is a variational statement and a generalization of the principle of virtual work to dynamics, is defined by [31]

$$0 = \int_{t_1}^{t_2}\left(\delta U + \delta W - \delta K\right)\mathrm{d}t \tag{16}$$

which after substituting Eqs. (10), (14) and (15) becomes

$$\begin{aligned}
0 = \int_{t_1}^{t_2}\int_{\Omega}\Big[&-\left(M_x + Y_{xy}\right)\delta w_{,xx} + \left(2M_{xy} + Y_x - Y_y\right)\delta w_{,xy} - \left(M_y - Y_{xy}\right)\delta w_{,yy} \\
&+\left(N_x w_{,x} + N_{xy} w_{,y}\right)\delta w_{,x} + \left(N_{xy} w_{,x} + N_y w_{,y}\right)\delta w_{,y} - \rho\left(\mathbf{x}\right)\dot{w}\delta\dot{w}\Big]\mathrm{d}\Omega\mathrm{d}t \\
&+\int_{\Omega}\left[N_x\delta u_{,x} + N_{xy}\delta u_{,y} + N_{xy}\delta v_{,x} + N_y\delta v_{,y} + Y_{xz}\frac{1}{2}\left(\delta v_{,xx} - \delta u_{,xy}\right) + Y_{yz}\frac{1}{2}\left(\delta v_{,xy} - \delta u_{,yy}\right)\right]\mathrm{d}\Omega \\
&-\int_{\Gamma}\left(\tilde{N}_n u_n + \tilde{N}_{nt} u_t\right)\mathrm{d}s + \int_{t_1}^{t_2}\left[-\int_{\Omega} g\left(\mathbf{x},t\right)\delta w \mathrm{d}\Omega + \int_{\Gamma}\tilde{M}_{nn}\delta w_{,n}\,\mathrm{d}s - \int_{\Gamma}\tilde{V}_n\delta w \mathrm{d}s\right]\mathrm{d}t.
\end{aligned} \tag{17}$$

Using the algebra of calculus of variations [31], taking into account that the membrane forces are not influenced by the stretching of the middle surface (linear plate theory) [34] and performing the necessary integrations by parts, we obtain the following: (i) boundary value problem, for the plane stress problem of the plate:

$$N_{x,x} + N_{xy,y} + \frac{1}{2}\left(Y_{xz,xy} + Y_{yz,yy}\right) = 0, \tag{18.1}$$

$$N_{xy,x} + N_{y,y} - \frac{1}{2}\left(Y_{xz,xx} + Y_{yz,xy}\right) = 0 \tag{18.2}$$

in Ω, together with the boundary conditions

$$N_x n_x^2 + N_y n_y^2 + 2N_{xy} n_x n_y + \frac{1}{2}\left(Y_{xz,y}\, n_x^2 - Y_{yz,x}\, n_y^2\right) + \frac{1}{2}\left(Y_{yz,y} - Y_{xz,x}\right) n_x n_y = \tilde{N}_n \quad \text{or}$$

$$u_n = \tilde{u}_n \quad \text{on} \quad \Gamma, \tag{19.1}$$

$$\left(N_y - N_x\right) n_x n_y + N_{xy}\left(n_x^2 - n_y^2\right) - \frac{1}{2}\left(Y_{yz,x} + Y_{xz,y}\right) n_x n_y - \frac{1}{2}\left(Y_{xz,x}\, n_x^2 + Y_{yz,y}\, n_y^2\right) = \tilde{N}_{nt} \quad \text{or}$$

$$u_t = \tilde{u}_t \quad \text{on} \quad \Gamma, \tag{19.2}$$

$$\frac{1}{2}Y_{yz} n_y^2 + \frac{1}{2}Y_{xz} n_x n_y = 0 \quad \text{or} \quad u_{,n} = 0 \quad \text{on} \quad \Gamma, \tag{19.3}$$

$$\frac{1}{2}Y_{xz} n_x^2 + \frac{1}{2}Y_{yz} n_x n_y = 0 \quad \text{or} \quad v_{,n} = 0 \quad \text{on} \quad \Gamma, \tag{19.4}$$

$$\frac{1}{2}Y_{xz} n_y^2 - \frac{1}{2}Y_{yz} n_x n_y = 0 \quad \text{or} \quad u_{,t} = 0 \quad \text{on} \quad \Gamma, \tag{19.5}$$

$$\frac{1}{2}Y_{yz} n_x^2 - \frac{1}{2}Y_{xz} n_x n_y = 0 \quad \text{or} \quad v_{,t} = 0 \quad \text{on} \quad \Gamma; \tag{19.6}$$

(ii) initial boundary value problem, for the bending vibration problem of the plate:

$$\rho(\mathbf{x})\, w_{,tt} - \left(M_x + Y_{xy}\right)_{,xx} + \left(2M_{xy} + Y_x - Y_y\right)_{,xy} - \left(M_y - Y_{xy}\right)_{,yy} - \left(N_x w_{,x} + N_{xy} w_{,y}\right)_{,x} - \left(N_{xy} w_{,x} + N_y w_{,y}\right)_{,y} - g(\mathbf{x}, t) = 0 \tag{20}$$

in Ω, together with the boundary conditions

$$Q_n - M_{nt,s} + N_n w_{,n} + N_{nt} w_{,t} = \tilde{V}_n \quad \text{or} \quad w = \tilde{w}, \tag{21.1}$$

$$M_{nn} = \tilde{M}_{nn} \quad \text{or} \quad w_{,n} = \tilde{w}_{,n} \tag{21.2}$$

on Γ and the corner condition

$$[\![M_{nt}]\!]_k = \tilde{R}_k \quad \text{or} \quad w_k = \tilde{w}_k \tag{22}$$

at the k-th corner and the initial conditions

$$w(\mathbf{x}, 0) = \tilde{w}(\mathbf{x}), \quad \dot{w}(\mathbf{x}, 0) = \dot{\tilde{w}}(\mathbf{x}). \tag{23.1,2}$$

The tilde over a symbol designates a prescribed quantity.

In the above relations, N_n, N_{nt} and M_{nn}, M_{nt}, Q_n are boundary stress resultants defined by

$$N_n = N_x n_x^2 + N_y n_y^2 + 2N_{xy} n_x n_y, \tag{24.1}$$

$$N_{nt} = \left(N_y - N_x\right) n_x n_y + N_{xy}\left(n_x^2 - n_y^2\right), \tag{24.2}$$

$$M_{nn} = \left(M_x + Y_{xy}\right) n_x^2 + \left(M_y - Y_{xy}\right) n_y^2 - 2\left(M_{xy} + \frac{Y_x - Y_y}{2}\right) n_x n_y, \tag{25.1}$$

$$M_{nt} = \left(M_{xy} + \frac{Y_x - Y_y}{2}\right)\left(n_x^2 - n_y^2\right) + \left(M_x - M_y + 2Y_{xy}\right) n_x n_y, \tag{25.2}$$

$$Q_n = \frac{\partial M_{nn}}{\partial n} - \frac{\partial M_{nt}}{\partial t} \tag{25.3}$$

where n, t denote the directions normal and tangent to the plate, respectively, $w_{,n}$,$w_{,t}$ the derivatives of the deflection w along the aforementioned directions, and n_x, n_y are the direction cosines of the outward normal vector. Equations (25) using Equations (13) become

$$M_{nn} = f_1 \nabla^2 w + f_2 w_{,nt} + (f_3 - f_1) w_{,tt}, \tag{26.1}$$

$$M_{nt} = g_1 \nabla^2 w + g_2 w_{,nt} + (g_3 - g_1) w_{,tt}, \tag{26.2}$$

$$Q_n = f_1 \left(\nabla^2 w\right)_{,n} + (f_3 - f_1 - g_2) w_{,ntt} + (f_2 - g_1)\left(\nabla^2 w\right)_{,t} + (g_1 - g_3 - f_2) w_{,ttt} \tag{26.3}$$

where f_1, f_2, f_3 and g_1, g_2, g_3 are given in the "Appendix".

Since we treat the linear buckling problem, the in-plane forces N_x, N_y, N_{xy} are known a priori as they are established by solving independently the plane stress problem of the plate described by Eqs. (18) and (19). This problem is solved using the AEM [31] after writing Eqs. (18) and (19) in terms of the displacements using Eqs. (12) and (13).

Introducing Eqs. (12) and (13) into Eq. (20) yields the following equation of motion in terms of the deflection:

$$\rho w_{,tt} + \left(D_{11} + D^l\right) w_{,xxxx} + 2\left(D_3 + D^l\right) w_{,xxyy} + \left(D_{22} + D^l\right) w_{,yyyy} - \left(N_x w_{,x} + N_{xy} w_{,y}\right)_{,x} - \left(N_{xy} w_{,x} + N_y w_{,y}\right)_{,y} = g(\mathbf{x}, t) \tag{27}$$

in Ω, where $D_3 = D_{12} + 2D_{66}$. The boundary conditions (21) can be rewritten in the most general form, including elastic support or restraint, as

$$\beta_1 w + \beta_2 \left(V_n + N_n w_{,n} + N_{nt} w_{,t}\right) = \beta_3, \tag{28.1}$$

$$\gamma_1 w_{,n} + \gamma_2 M_{nn} = \gamma_3 \tag{28.2}$$

where β_i and γ_i are functions specified on Γ and $V_n = Q_n - M_{nt,s}$ is the effective shear force which for straight sides ($M_{nt,s} = M_{nt,t}$) is given by

$$V_n = f_1 \left(\nabla^2 w\right)_{,n} + (f_3 - f_1 - 2g_2)\, w_{,ntt} + (f_2 - 2g_1) \left(\nabla^2 w\right)_{,t} + (2g_1 - 2g_3 - f_2)\, w_{,ttt}\,. \tag{29}$$

Note that all conventional boundary conditions can be derived from Eqs. (28) by specifying appropriately the β_i and γ_i functions. When the boundary Γ is nonsmooth, the following corner condition:

$$a_{1k} w_k + a_{2k} [\![M_{nt}]\!]_k = a_{3k}, \quad a_{2k} \neq 0 \tag{30}$$

must be added to Eqs. (28), in which a_{ik} are constants specified at the k-th corner. One can observe that setting $D^l = 0$, Eqs. (27), (28) and (30) yield the governing equation and the boundary conditions of the orthotropic Kirchhoff plate theory [35].

2.1 Free vibrations of orthotropic micro-plates

The equation of motion for the free vibration problem of an orthotropic micro-plate is derived from Eq. (27) in the absence of external transverse loading $g(\mathbf{x}, t) = 0$, that is

$$\begin{aligned} \rho w_{,tt} + \left(D_{11} + D^l\right) w_{,xxxx} + 2\left(D_3 + D^l\right) w_{,xxyy} + \left(D_{22} + D^l\right) w_{,yyyy} \\ - \left(N_x w_{,x} + N_{xy} w_{,y}\right)_{,x} - \left(N_{xy} w_{,x} + N_y w_{,y}\right)_{,y} = 0 \end{aligned} \tag{31}$$

in Ω, together with the homogeneous boundary conditions (28)

$$\beta_1 w + \beta_2 \left(V_n + N_n w_{,n} + N_{nt} w_{,t}\right) = 0, \tag{32.1}$$

$$\gamma_1 w_{,n} + \gamma_2 M_{nn} = 0 \tag{32.2}$$

on the boundary Γ.

2.2 Buckling of orthotropic micro-plates

The differential equation for linear buckling of an orthotropic micro-plate is derived also from Eq. (27) by setting the external transverse loading $g(\mathbf{x}, t) = 0$ and considering homogeneous boundary conditions. Thus, if the in-plane membrane forces are expressed in terms of a parameter λ, namely

$$N_x = \lambda \tilde{N}_x, \quad N_y = \lambda \tilde{N}_y, \quad N_{xy} = \lambda \tilde{N}_{xy} \tag{33}$$

the buckling problem for constant membrane forces is described by the following equation:

$$\begin{aligned} \left(D_{11} + D^l\right) w_{,xxxx} + 2\left(D_3 + D^l\right) w_{,xxyy} + \left(D_{22} + D^l\right) w_{,yyyy} \\ - \lambda \left(\tilde{N}_x w_{,xx} + 2\tilde{N}_{xy} w_{,xy} + \tilde{N}_y w_{,yy}\right) = 0 \end{aligned} \tag{34}$$

in Ω, together with the boundary conditions

$$\beta_1 w + \beta_2 \left(V_n + N_n w_{,n} + N_{nt} w_{,t}\right) = 0, \tag{35.1}$$

$$\gamma_1 w_{,n} + \gamma_2 M_{nn} = 0 \tag{35.2}$$

on the boundary Γ.

2.3 Bending of orthotropic micro-plates

Finally, the differential equation for linear bending of orthotropic micro-plates is deduced from Eq. (27). Neglecting the inertia terms, in the absence of in-plane membrane forces, yields the equation [22]

$$\left(D_{11} + D^l\right) w_{,xxxx} + 2\left(D_3 + D^l\right) w_{,xxyy} + \left(D_{22} + D^l\right) w_{,yyyy} = g(\mathbf{x}) \tag{36}$$

in Ω, together with the boundary conditions (28).

3 The AEM solution

Several BEM techniques have been reported in the literature, treating the bending problem of thin orthotropic and anisotropic plates [36–38]. In this paper, the AEM is employed to solve the initial boundary value problem described by Eqs. (27), (28) and (23). Let w be the sought solution to Eq. (27). This function is four times continuously differentiable with respect to the co-ordinates x, y in Ω and three times on its boundary Γ. According to the AEM of Katsikadelis [39], as it was developed for plates [40–42], Eq. (27) can be replaced by the biharmonic equation

$$\nabla^4 w = b\,(\mathbf{x}, t) \tag{37}$$

where $b\,(\mathbf{x}, t)$ is the unknown fictitious load. Eq. (37) is quasi-static, that is, the time variable appears as a parameter. It indicates that the solution of Eq.(27) can be obtained as the deflection surface of an isotropic plate with unit stiffness subjected to the fictitious time-dependent load $b\,(\mathbf{x}, t)$ under the given boundary and initial conditions.

According to the AEM, the unknown fictitious load $b\,(\mathbf{x}, t)$ can be established using BEM as following. For the function w satisfying Eq. (37), the following two integral representations are obtained [41]:

$$cw(\mathbf{x}, t) = \int_\Omega \Lambda_4 b\,(\mathbf{x}, t)\,\mathrm{d}\Omega - \int_\Gamma \left[\Lambda_1 w + \Lambda_2 w_{,n} + \Lambda_3 \nabla^2 w + \Lambda_4 (\nabla^2 w)_{,n}\right] \mathrm{d}s, \tag{38}$$

$$c\nabla^2 w(\mathbf{x}, t) = \int_\Omega \Lambda_2 b\,(\mathbf{x}, t)\,\mathrm{d}\Omega - \int_\Gamma \left[\Lambda_1 \nabla^2 w + \Lambda_2 (\nabla^2 w)_{,n}\right] \mathrm{d}s \tag{39}$$

where $c = 2\pi, \pi,\ 0$ depending on if $\mathbf{x} \in \Omega$, $\mathbf{x} \in \Gamma$, $\mathbf{x} \notin \Omega \cup \Gamma$, respectively. Note that the boundary has been assumed to be smooth at the point $\mathbf{x}$. The kernels $\Lambda_i = \Lambda_i\,(\mathbf{r})$, with $\mathbf{r} = |\mathbf{x} - \boldsymbol{\xi}|$ being the distance between the field point $\mathbf{x} \in \Omega \cup \Gamma$ and source point $\boldsymbol{\xi} \in \Gamma$, corresponding to the fundamental solution of Eq. (37) are given as [41]

$$\Lambda_1\,(r) = -\frac{\cos\varphi}{r}, \quad \Lambda_2\,(r) = \ln r + 1, \tag{40.1,2}$$

$$\Lambda_3\,(r) = -\frac{1}{4}\,(2r\ln r + r)\cos\varphi, \quad \Lambda_4\,(r) = \frac{1}{4} r^2 \ln r \tag{40.3,4}$$

where $\varphi = \measuredangle \mathbf{r}, \mathbf{n}$.

The derivatives of the deflection up to the third order for points $\mathbf{x} \in \Omega$ are obtained by direct differentiation of Eq. (38). Thus, for the sake of conciseness, we can write the integral representations of the deflection and its derivatives at a point $\mathbf{x} \in \Omega$ as

$$\begin{aligned} 2\,\pi\, w_{,pqr}\,(\mathbf{x}, t) = &\int_\Omega \Lambda_{4,pqr}\, b\,(\mathbf{x}, t)\, d\Omega \\ &- \int_\Gamma \left[\Lambda_{1,pqr}\, w + \Lambda_{2,pqr}\, w_{,n} + \Lambda_{3,pqr}\, \nabla^2 w + \Lambda_{4,pqr}\, (\nabla^2 w)_{,n}\right] ds \end{aligned} \tag{41}$$

where $p, q, r = 0, x, y$. The derivatives of the kernels are given in [41].

On the basis of Eqs. (21.1), (26) and (29), the boundary conditions (28) are written as

$$\begin{aligned} &\beta_1 w + \beta_2 \left[f_1 \left(\nabla^2 w\right)_{,n} + (f_3 - f_1 - 2g_2)\, w_{,ntt} + (f_2 - 2g_1) \left(\nabla^2 w\right)_{,t}\right. \\ &\left. + (2g_1 - 2g_3 - f_2)\, w_{,ttt} + \tilde{N}_n w_{,n} + \tilde{N}_{nt} w_{,t}\right] = \beta_3, \end{aligned} \tag{42.1}$$

$$\gamma_1 w_{,n} + \gamma_2 \left[f_1 \nabla^2 w + f_2 w_{,nt} + (f_3 - f_1)\, w_{,tt}\right] = \gamma_3. \tag{42.2}$$

The integral representations (38) and (39) for $\mathbf{x} \in \Gamma$ together with the boundary conditions (42) constitute a set of four equations (two integral and two differential) with respect to the four boundary quantities w, $w_{,n}$, $\nabla^2 w$ and $(\nabla^2 w)_{,n}$. The system is solved numerically using the BEM for the integral equations and the finite difference method for the differential equations [40–42]. Thus, the boundary of the plate is divided into N

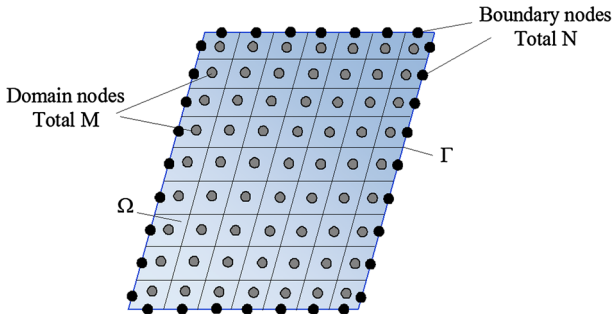

Fig. 2 Boundary and domain discretization

constant boundary elements and the domain into M quadrilateral elements on which the unknown quantities are assumed constant (see Fig. 2). Subsequently, the four boundary quantities can be eliminated from the discretized part of Eqs. (41), which yields

$$\mathbf{w} = \mathbf{W}_0\mathbf{b} + \mathbf{w}_0, \tag{43.1}$$

$$\mathbf{w}_{,pqr} = \mathbf{W}_{0pqr}\mathbf{b} + \mathbf{w}_{0pqr} \tag{43.2}$$

where $\mathbf{W}_0$, $\mathbf{W}_{0pqr}$ are known $M \times M$ matrices and $\mathbf{w}_0$, $\mathbf{w}_{0pqr}$ are known $M \times 1$ vectors emanating when nonhomogeneous boundary conditions exist (i.e., $\beta_3 \neq 0$, $\gamma_3 \neq 0$).

The regular domain integrals in Eq. (41) are computed using the Gauss method with nine internal integration points. Domain singular and hyper-singular integrals in Eq. (41) arise when the domain source (collocation) point coincides with the domain field point. This computation can be effectively done by converting the domain singular integrals over a domain cell into regular integrals along its boundary using Green's reciprocal identity as in [41,42].

Furthermore, the derivatives of the deflection with respect to time can be obtained by direct differentiation of Eq. (43.1). That is,

$$\dot{\mathbf{w}} = \mathbf{W}_0\dot{\mathbf{b}} + \dot{\mathbf{w}}_0, \tag{44.1}$$

$$\ddot{\mathbf{w}} = \mathbf{W}_0\ddot{\mathbf{b}} + \ddot{\mathbf{w}}_0. \tag{44.2}$$

Note that the time derivatives of $\mathbf{w}_0$ appear only when the functions β_3, γ_3 depend on time as well.

The final step of AEM is to apply Eq. (27) to M domain nodal points inside Ω (see Fig. 2) and substitute the deflection and its derivatives on the basis of Eqs. (43) and (44). Thus, we obtain

$$\mathbf{M}\ddot{\mathbf{b}} + \mathbf{K}\mathbf{b} - \left(\mathbf{N_x}\mathbf{w}_{,xx} + 2\mathbf{N_{xy}}\mathbf{w}_{,xy} + \mathbf{N_y}\mathbf{w}_{,yy}\right) = \mathbf{g} \tag{45}$$

where $\mathbf{M}$ and $\mathbf{K}$ are known square matrices having dimension $M \times M$; $\mathbf{N_x}$, $\mathbf{N_y}$, $\mathbf{N_{xy}}$ are known diagonal $M \times M$ matrices containing the values of the constant membrane forces N_x, N_y, N_{xy}; $\mathbf{g}$ is a vector including the M values of the external load $g(\mathbf{x}, t)$ and $\mathbf{b}$ is the vector of the M values of the fictitious load $b(\mathbf{x}, t)$ to be determined. Subsequently, using Eq. (43.2) to replace the derivatives $\mathbf{w}_{,xx}$, $\mathbf{w}_{,xy}$, $\mathbf{w}_{,yy}$, an equation of the following form is obtained:

$$\mathbf{M}\ddot{\mathbf{b}} + (\mathbf{K} - \mathbf{F})\,\mathbf{b} = \mathbf{g} \tag{46}$$

with

$$\mathbf{F} = \mathbf{N_x}\mathbf{W}_{0xx} + 2\mathbf{N_{xy}}\mathbf{W}_{0xy} + \mathbf{N_y}\mathbf{W}_{0yy}. \tag{47}$$

Equation (46) is the semi-discretized equation of motion of the orthotropic plate with $\mathbf{M}$, $\mathbf{K}$ representing the generalized mass and stiffness matrices, respectively. It can be solved numerically, using any time-step integration technique to establish the time-dependent unknown fictitious load $\mathbf{b}$. The initial conditions of Eq. (46) are obtained from Eqs. (43.1) and (44.1) on the basis of Eqs. (23) as follows:

$$\mathbf{b}(0) = \mathbf{W}_0^{-1}(\tilde{\mathbf{w}} - \mathbf{w}_0), \tag{48.1}$$

$$\dot{\mathbf{b}}(0) = \mathbf{W}_0^{-1}(\dot{\tilde{\mathbf{w}}} - \dot{\mathbf{w}}_0). \tag{48.2}$$

3.1 Free vibrations of orthotropic plates

In this case, the equation of motion (46) takes the form

$$\mathbf{M}\ddot{\mathbf{b}} + (\mathbf{K} - \mathbf{F})\,\mathbf{b} = \mathbf{0}, \tag{49}$$

and by setting

$$\mathbf{b}(\mathbf{x}, t) = \mathbf{B}(\mathbf{x})e^{i\omega t} \tag{50}$$

Eq. (49) becomes

$$\left[(\mathbf{K} - \mathbf{F}) - \omega^2\mathbf{M}\right]\mathbf{B} = \mathbf{0}, \tag{51}$$

from which the eigenfrequencies and the mode shapes are established numerically by solving a typical eigenvalue problem of linear algebra.

3.2 Buckling of orthotropic plates

In this case, Eq. (34) takes the form

$$\mathbf{Kb} - \lambda\left(\mathbf{N_x}\mathbf{w}_{,xx} + 2\mathbf{N_{xy}}\mathbf{w}_{,xy} + \mathbf{N_y}\mathbf{w}_{,yy}\right) = \mathbf{0}. \tag{52}$$

Further, using Eq. (43.2) to replace the derivatives, the following equation is obtained:

$$(\mathbf{K} - \lambda\mathbf{F})\mathbf{b} = \mathbf{0} \tag{53}$$

where $\mathbf{F}$ is the known square $M \times M$ matrix given by Eq. (47).

The requirement that Eq. (53) has a nontrivial solution yields the buckling equation

$$\det(\mathbf{K} - \lambda\mathbf{F}) = 0. \tag{54}$$

3.3 Bending of orthotropic micro-plates

In this case, Eq. (36) takes the form

$$\mathbf{Kb} = \mathbf{g} \tag{55}$$

where $\mathbf{K}$ is a known $M \times M$ matrix, $\mathbf{g}$ is also a known $M \times 1$ vector including the M values of the external load $g(\mathbf{x})$, and $\mathbf{b}$ is the vector of the M values of the fictitious load $b(\mathbf{x})$ to be determined.

4 Numerical examples

On the basis of the numerical procedure presented in the previous section, a FORTRAN code has been written and numerical results for certain micro-plates have been obtained, which illustrate the applicability, effectiveness and accuracy of the proposed model.

4.1 Vibrations of an orthotropic skew micro-plate

As a first example, we consider a clamped orthotropic skew micro-plate with various aspect ratios (b/a) of the skew sides ($N = 100$, $M = 225$). In order to validate the proposed method, an orthotropic plate ($l = D^l = 0$) was first investigated. The data in this case are as follows: $D_{11} = 1$, $D_{22} = 0.25$ and $D_{12} + 2D_{66} = 1$. In Table 1, numerical results for the dimensionless frequency parameter $K_f = \omega a^2\sqrt{\rho h/D_{11}}$ of the plate are presented, which are in very good agreement as compared with those obtained by Sakata and Hayashi [43]. Subsequently, the response of the same plate was investigated taking into account the microstructural effect, as measured by the material length scale parameter l. Results for the frequency parameter are also presented in Table 1 and Fig. 3. It is apparent that the frequency parameter increases with increasing the value of the skew angle. This was also reported in [25,26] using the nonlocal elasticity theory. However, an important finding is that the frequency parameter increases nonlinearly by increasing the material length scale parameter of the modified couple stress theory, which is in direct contradiction to that of the nonlocal elasticity theory where the frequency parameter decreases by increasing the nonlocal parameter [25,26]. Finally, it is worth mentioning that the slope of the frequency parameter curve depends on the skew angle ψ, and particularly, the larger the skew angle, the steeper the slope.

Table 1 Frequency parameter K_f of the orthotropic skew micro-plates of Example 4.1

$(b/a)\cos\varphi/\varphi$	[43]	$l/h=0$	$l/h=0.1$	$l/h=0.2$	$l/h=0.3$	$l/h=0.4$
0.5/80	23.7746	23.7348	24.2423	25.7037	27.9682	30.8591
1.0/70	25.8101	25.8881	26.4438	28.0443	30.5252	33.6962
1.5/60	29.5859	29.7017	30.3646	32.2702	35.2152	38.9639
2.0/50	35.9342	35.8078	36.6966	39.2414	43.1485	48.0861
2.5/40	46.8856	47.1281	48.4700	52.2862	58.0855	65.3389
3.0/30	68.2991	68.8298	71.3064	78.2598	88.6309	101.3700

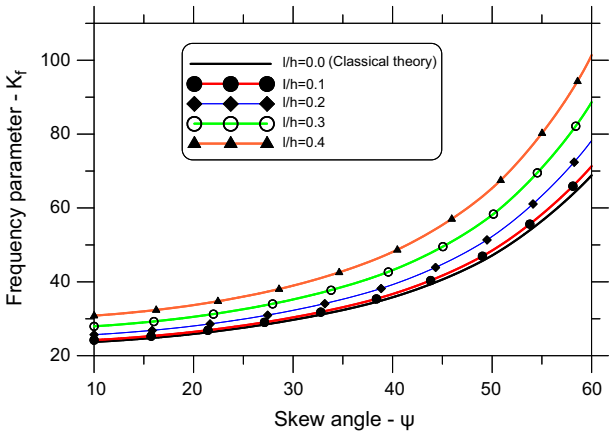

Fig. 3 Frequency parameter K_f versus the skew angle ψ

Table 2 Eigenfrequencies ω_i of the orthotropic square micro-plate of Example 4.2

ω_i	[44]	$l/h=0$	$l/h=0.1$	$l/h=0.2$	$l/h=0.3$	$l/h=0.4$
1	17.860	17.543	18.432	20.697	23.745	27.258
2	36.295	36.034	37.326	40.921	46.228	52.708
3	45.683	45.660	47.920	53.832	62.111	71.983
4	67.071	68.191	70.600	77.118	86.421	97.517
5	74.466	76.023	77.802	82.873	90.612	100.347

4.2 Vibrations of an orthotropic square micro-plate

In order to demonstrate the efficacy of the method to treat plates with complex boundary conditions, the vibration of an orthotropic square micro-plate with a free edge, while the others are clamped, has been analyzed ($N=100$, $M=225$). The data in this case are as follows: $D_{11}=2$, $D_{22}=1$, $D_{12}=0.6$ and $D_{66}=2/3$. In Table 2, the first five eigenfrequencies ω_i of the plate are presented and compared favorably with those obtained by Rossi et al. [44] ($l=D^l=0$). Afterward, the same plate was investigated taking into account the microstructural effect, as measured by the material length scale parameter l. Results for the first five eigenfrequencies ω_i of the plate are also presented in Table 2. As it was anticipated, all the eigenfrequencies increase with the increase of the material length scale parameter l.

4.3 Buckling of an orthotropic skew micro-plate

The third example is devoted to the buckling of a simply supported orthotropic skew micro-plate with equal length sides ($a=b$, $N=100$, $M=225$). The plate is subjected to a uniform compressive load $\tilde{N}_x$ as depicted in Fig. 4. In this case, the data are as follows: $D_{11}=1=D$, $D_{22}=5.6025D$, $D_{12}=0.375D$ and $D_{66}=0.9375D$. In Table 3 and Fig. 5, results for the critical load parameter $K_b=N_{cr}b^2/\pi^2D_{11}$ are presented taking into account the microstructural effect. It can be observed that the critical load parameter increases also nonlinearly with increasing the material length scale parameter. This is also in direct contradiction to that of the nonlocal elasticity theory where the critical load parameter decreases by increasing the nonlocal parameter

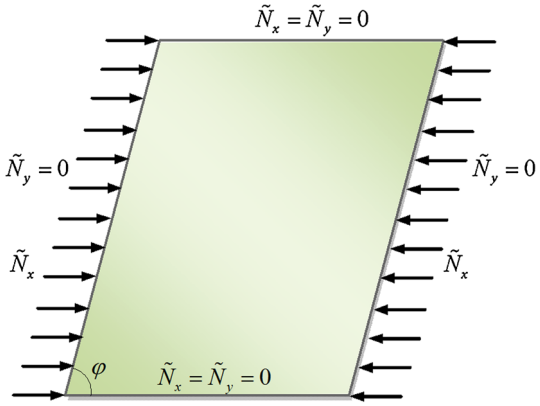

Fig. 4 Skew plate under uniform uniaxial compression

Table 3 Critical load parameter K_b of the orthotropic skew micro-plates of Example 4.3

φ	$l/h = 0$	$l/h = 0.1$	$l/h = 0.2$	$l/h = 0.3$	$l/h = 0.4$
90	10.2421	10.9518	13.0806	15.3761	18.5385
75	11.4186	12.1943	14.5136	17.1068	20.6160
60	15.5549	16.5713	19.4618	23.0961	27.9851
45	25.6315	27.0121	31.0003	37.3069	45.7409

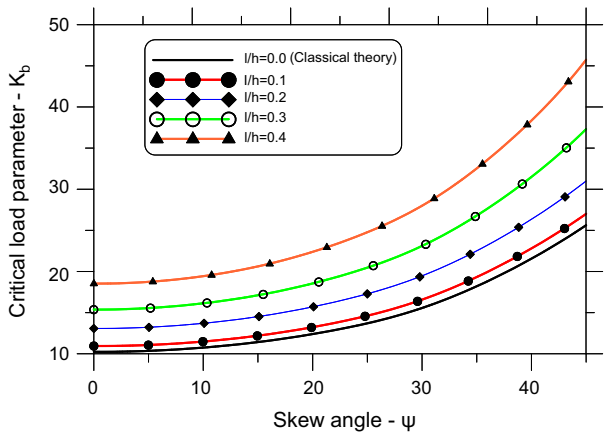

Fig. 5 Critical load parameter K_b versus the skew angle ψ

[21]. From Fig. 5, it can be pointed out that the rate of change of the critical load parameter also increases by increasing the skew angle ψ.

4.4 Bending of a clamped orthotropic skew micro-plate

In this final example, the bending of a clamped with equal length sides ($a = b$) orthotropic skew micro-plate is considered ($N = 100, M = 225$). First, an orthotropic plate ($l = D^l = 0$) was investigated in order to compare the results with those available in the literature obtained by Hadid and Bashir [45]. The data in this case are as follows: $D_{11} = 4, D_{22} = 1, D_{12} = 0.30$ and $D_{66} = 0.35$. By comparing from Table 4, the evaluated normalized central deflection $\bar{w} = wD_{22}10^3/[g(a/2)^4]$ and maximum positive moment $\bar{M} = M \times 10/[g \times (a/2)^2]$ with the available ones, it can be pointed out that the results are in very good agreement. Further, the influence of the microstructural effect on the same plate was investigated. The normalized central deflection and maximum positive moment for various values of the l/h ratio are also presented in Table 4 and Figs. 6 and 7. It can be easily detected that both the normalized central deflection and maximum positive moment of the micro-plate decrease nonlinearly with increasing the material length scale parameter.

Table 4 Normalized central deflection and maximum positive moment of the orthotropic skew micro-plates of Example 4.4

φ	[45]		$l/h=0$		$l/h=0.1$		$l/h=0.2$		$l/h=0.3$		$l/h=0.4$	
	$\bar{w}$	$\bar{M}$	$\bar{w}$	$\bar{M}$	$\bar{w}$	$\bar{M}$	$\bar{w}$	$\bar{M}$	$\bar{w}$	$\bar{M}$	$\bar{w}$	$\bar{M}$
75	8.656	1.435	8.619	1.427	8.452	1.400	7.984	1.325	7.309	1.215	6.533	1.086
60	6.854	1.177	6.987	1.195	6.822	1.164	6.371	1.081	5.740	0.964	5.042	0.835
45	4.086	0.775	3.998	0.759	3.885	0.733	3.583	0.662	3.173	0.566	2.737	0.464
30	1.390	0.343	1.336	0.337	1.344	0.344	1.192	0.289	1.001	0.222	0.811	0.158

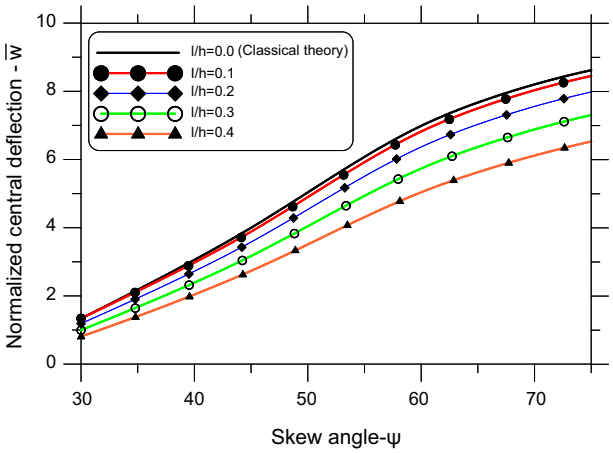

Fig. 6 Normalized central deflection $\bar{w}$ versus the skew angle ψ

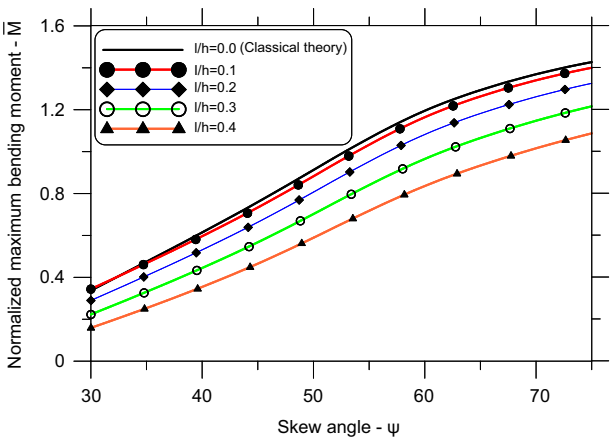

Fig. 7 Normalized maximum positive moment $\bar{M}$ versus the skew angle ψ

5 Conclusions

In this paper the response of an orthotropic skew micro-plate was studied based on a modified couple stress theory containing only one material length scale parameter. Using Hamilton's principle, the governing equilibrium equation of the micro-plate and the associated general boundary conditions are derived in terms of the deflection. The resulting initial boundary value problem is solved employing the AEM. The main conclusions that can be drawn from this investigation are as follows:

(i) The present formulation is capable of capturing the size effect on the investigation of orthotropic Kirchhoff-type skew micro-plates and is alleviated from fundamental flaws in existing micro-plate models, which contain more than one material length scale parameter.

(ii) In the vibration case, the frequency parameter increases with an increase of the value of the skew angle. This finding was also verified using the nonlocal elasticity theory. In addition, the frequency parameter of the micro-plate increases nonlinearly with increasing the material length scale parameter. Moreover, the

slope of the frequency parameter curve depends on the skew angle Ψ, and particularly, the larger the skew angle, the steeper the slope.

(iii) In the buckling case, the critical load parameter of the micro-plate increases nonlinearly with a linear increase of the value of the material length scale parameter. Further, the rate of change of the critical load parameter also increases with increasing the skew angle.

(iv) In the bending case, both the central deflection and maximum positive moment of the micro-plate decrease nonlinearly with the increase of the material length scale parameter.

(v) A new important finding is that both the frequency and critical load parameters increase with increasing the material length scale parameter of the modified couple stress theory, which is in direct contradiction to that of the nonlocal elasticity theory where these parameters decrease with increasing the nonlocal parameter.

6 Appendix

The values of the parameters f_1, f_2, f_3 and g_1, g_2, g_3 are given as:

$$f_1 = -\left(D_{11} + D^l\right) n_x^4 - 2\left(D_3 + D^l\right) n_x^2 n_y^2 - \left(D_{22} + D^l\right) n_y^4, \tag{A1}$$

$$f_2 = 2\left[D_{11} n_x^2 - D_{22} n_y^2 - D_3\left(n_x^2 - n_y^2\right)\right] n_x n_y, \tag{A2}$$

$$f_3 = -D_{12} + D^l - \left(D_{11} + D_{22} - 2D_3\right) n_x^2 n_y^2, \tag{A3}$$

$$g_1 = \left[-D_{11} n_x^2 + D_{22} n_y^2 + D_3\left(n_x^2 - n_y^2\right)\right] n_x n_y = -\frac{1}{2} f_2, \tag{A5}$$

$$g_2 = 2\left(D_{66} + D^l\right) + 2\left(D_{11} - D_{22} - 2D_3\right) n_x^2 n_y^2, \tag{A6}$$

$$g_3 = \left[-D_{11} n_y^2 + D_{22} n_x^2 - D_3\left(n_x^2 - n_y^2\right)\right] n_x n_y. \tag{A7}$$

References

1. Lam, D.C.C., Yang, F., Chong, A.C.M., Wang, J., Tong, P.: Experiments and theory in strain gradient elasticity. J. Mech. Phys. Solids **51**, 1477–1508 (2003)
2. Narendar, S., Gopalakrishnan, S.: Scale effects on buckling analysis of orthotropic nanoplates based on nonlocal two-variable refined plate theory. Acta Mech. **223**, 395–413 (2012)
3. Papargyri-Beskou, S., Giannakopoulos, A.E., Beskos, D.E.: Variational analysis of gradient elastic flexural plates under static loading. Int. J. Solids Struct. **47**, 2755–2766 (2010)
4. Lu, P., Zhang, P.Q., Lee, H.P., Wang, C.M., Reddy, J.N.: Non-local elastic plate theories. Proc. R. Soc. A **463**, 3225–3240 (2007)
5. Tsiatas, G.C.: A new Kirchhoff plate model based on a modified couple stress theory. Int. J. Solids Struct. **46**, 2757–2764 (2009)
6. Lazopoulos, K.A.: On bending of strain gradient elastic micro-plates. Mech. Res. Commun. **36**, 777–783 (2009)
7. Yin, L., Qian, Q., Wang, L., Xia, W.: Vibration analysis of microscale plates based on modified couple stress theory. Acta Mech. Solida Sin. **23**, 386–393 (2010)
8. Jomehzadeh, E., Noori, H.R., Saidi, A.R.: The size-dependent vibration analysis of microplates based on a modified couple stress theory. Physica E **43**, 877–883 (2011)
9. Mohammadi, M., Ghayour, M., Farajpou r., A.: Free transverse vibration analysis of circular and annular graphene sheets with various boundary conditions using the nonlocal continuum plate model. Compos. Part B Eng. **45**, 32–42 (2013)
10. Eringen, A.C.: On differential equations of nonlocal elasticity and solutions of screw dislocation and surface waves. J. Appl. Phys. **54**, 4703-1470 (1983)
11. Sakhaee-Pour, A.: Elastic buckling of single-layered graphene sheet. Comp. Mater. Sci. **45**, 266–270 (2009)
12. Pradhan, S.C., Phadikar, J.K.: Small scale effect on vibration of embedded multilayered graphene sheets based on nonlocal continuum models. Phys. Lett. A **373**, 1062–1069 (2009)

13. Murmu, T., Pradhan, S.C.: Buckling of biaxially compressed orthotropic plates at small scales. Mech. Res. Commun. **36**, 933–938 (2009)
14. Pouresmaeeli, S., Fazelzadeh, S.A., Ghavanloo, E.: Exact solution for nonlocal vibration of double-orthotropic nanoplates embedded in elastic medium. Compos. Part B Eng. **43**, 3384–3390 (2012)
15. Satish, N., Narendar, S., Gopalakrishnan, S.: Thermal vibration analysis of orthotropic nanoplates based on nonlocal continuum mechanics. Physica E **44**, 1950–1962 (2012)
16. Pouresmaeeli, S., Ghavanloo, E., Fazelzadeh, S.A.: Vibration analysis of viscoelastic orthotropic nanoplates resting on viscoelastic medium. Compos. Struct. **96**, 405–410 (2013)
17. Pradhan, S.C., Kumar, A.: Vibration analysis of orthotropic graphene sheets embedded in Pasternak elastic medium using nonlocal elasticity theory and differential quadrature method. Comput. Mater. Sci. **50**, 239–245 (2010)
18. Pradhan, S.C., Kumar, A.: Vibration analysis of orthotropic graphene sheets using nonlocal elasticity theory and differential quadrature method. Compos. Struct. **93**, 774–779 (2011)
19. Farajpour, A., Shahidi, A.R., Mohammadi, M., Mahzoon, M.: Buckling of orthotropic micro/nanoscale plates under linearly varying in-plane load via nonlocal continuum mechanics. Compos. Struct. **94**, 1605–1615 (2012)
20. Shahidi, A.R., Anjomshoa, A., Shahidi, S.H., Kamrani, M.: Fundamental size dependent natural frequencies of non-uniform orthotropic nano scaled plates using nonlocal variational principle and finite element method. Appl. Math. Model. **37**, 7047–7061 (2013)
21. Analooei, H.R., Azhari, M., Heidarpour, A.: Elastic buckling and vibration analyses of orthotropic nanoplates using nonlocal continuum mechanics and spline finite strip method. Appl. Math. Model. **37**, 6703–6717 (2013)
22. Tsiatas, G.C., Yiotis, A.J. : A microstructure-dependent orthotropic plate model based on a modified couple stress theory. In: Sapountzakis, E. (ed.) Recent Developments in Boundary Element Methods, A Volume to Honour Professor John T. Katsikadelis, WIT Press, Southampton (2010)
23. Yang, F., Chong, A.C.M, Lam, D.C.C, Tong, P.: Couple stress based strain gradient theory of elasticity. Int. J. Solids Struct. **39**, 2731–2743 (2002)
24. Park, S.K., Gao, X.-L.: Variational formulation of a modified couple stress theory and its application to a simple shear problem. Z. Angew. Math. Phys. **59**, 904–917 (2008)
25. Malekzadeh, P., Setoodeh, A.R., Alibeygi Beni, A.: Small scale effect on the free vibration of orthotropic arbitrary straight-sided quadrilateral nanoplates. Compos. Struct. **93**, 1631–1639 (2011)
26. Beni Alibeygi, A., Malekzadeh, P.: Nonlocal free vibration of orthotropic non prismatic skew nanoplates. Compos. Struct. **94**, 3215–3222 (2012)
27. Antoine, A.: Effect of couple-stresses on the elastic bending of beams. Int. J. Solids Struct. **37**, 1003–1018 (2000)
28. Chen, W., Li, X.: A new modified couple stress theory for anisotropic elasticity and microscale laminated Kirchhoff plate model. Arch. Appl. Mech. **84**, 323–341 (2014)
29. Koiter, W.T.: Couple stresses in the theory of elasticity, I and II. Proc. K Ned. Akad. Wet. (B) **67**, 17–44 (1964)
30. Santos, J.V.A.D., Reddy, J.N.: Vibration of Timoshenko beams using non-classical elasticity theories. Shock. Vib. **19**, 251–256 (2012)
31. Katsikadelis, J.T.: The boundary element method for plate analysis. 1st edn. Academic Press, Oxford (2014)
32. Rand, O., Rovenski, V.: Analytical Methods in Anisotropic Elasticity: with symbolic computational tools. Birkhäuser, Boston (2004)
33. Reddy, J.N.: Energy principles and variational methods in applied mechanics, 2nd edn. Wiley, New York (2002)
34. Babouskos, N., Katsikadelis, J.T.: Flutter instability of damped plates under combined conservative and nonconservative loads. Arch. Appl. Mech. **79**, 541–556 (2009)
35. Tsiatas, G.C., Yiotis, A.J.: A BEM-based meshless solution to buckling and vibration problems of orthotropic plates. Eng. Anal. Bound. Elem. **37**, 579–584 (2013)
36. Irschik, H.: A boundary-integral equation method for bending of orthotropic plates. Int. J. Solids Struct. **37**, 245–255 (1984)
37. Shi, G., Bezine, G.: A general boundary integral formulation for the anisotropic plate bending problems. J. Compos. Mater. **22**, 694–716 (1988)
38. Albuquerque, E.L., Sollero, P., Venturini, W.S., Aliabadi, M.H.: Boundary element analysis of anisotropic Kirchhoff plates. Int. J. Solid. Struct. **43**, 4029–4046 (2006)
39. Katsikadelis, J.T.: The analog equation method-a powerful BEM-based solution technique for solving linear and nonlinear engineering problems. In: Brebbia, C.A. (ed.) Boundary elements VI, CLM publications, Southampton (1994)
40. Katsikadelis, J.T, Armenakas, A.E.: A new boundary equation solution to the plate problem. J. Appl. Mech. ASME **56**, 364–374 (1989)
41. Nerantzaki, M.S., Katsikadelis, J.T.: An analog equation solution to dynamic analysis of plates with variable thickness. Eng. Anal. Bound. Elem. **17**, 145–152 (1996)
42. Nerantzaki, M.S., Katsikadelis, J.T.: Buckling of plates with variable thickness—an analog equation solution. Eng. Anal. Bound. Elem. **18**, 149–154 (1996)
43. Sakata, T., Hayashi, T.: Natural frequencies of clamped orthotropic skew plates. J. Sound. Vib. **81**, 287–298 (1982)
44. Rossi, R.E., Bambill, D.V., Laura, P.A.A.: Vibrations of a rectangular orthotropic plate with a free edge: a comparison of analytical and numerical results. Ocean Eng. **25**, 521–527 (1998)
45. Hadid, H.A., Bashir, M.H.M.: Analysis of orthotropic thin plate using spline-integral method. Comput. Struct. **37**, 423–428 (1990)